

DEVELOPMENT OF A 2D BIOMECHANICAL MODEL TO SIMULATE SEATED MULTIDIRECTIONAL ARM STRENGTH OF PEOPLE WITH C5-C7 TETRAPLEGIA

Stilwell, George;
Symons, Digby;
Gooch, Shayne

University of Canterbury

ABSTRACT

People living with tetraplegia experience a significant loss of sensory and motor function; with the severity depending on their injury level and completeness. To complete tasks independently, people with tetraplegia often rely on assistive devices. To avoid upper extremity pain, designs should not require applications of force near the limits of the user's physical strength. This paper establishes a 2D biomechanical model using static equilibrium and joint torque limits to predict multidirectional strength patterns in the sagittal plane for people with C5 to C7 tetraplegia in a seated position. The results from the biomechanical model highlight the areas and directions of high strength. The strength patterns observed in this paper provide an opportunity for designers to evaluate strength requirements and take advantage of areas and directions of high strength and ensure that users are not required to apply force near their physical limit. In doing this, designs such as assistive devices can be developed that enable users with a reduction in strength to operate them independently.

Keywords: Inclusive design, Evaluation, Simulation, Human model, Tetraplegia

Contact:

Stilwell, George
UC
New Zealand
george.stilwell@canterbury.ac.nz

Cite this article: Stilwell, G., Symons, D., Gooch, S. (2023) 'Development of a 2D Biomechanical Model to Simulate Seated Multidirectional Arm Strength of People with C5-C7 Tetraplegia', in *Proceedings of the International Conference on Engineering Design (ICED23)*, Bordeaux, France, 24-28 July 2023. DOI:10.1017/pds.2023.144

1 INTRODUCTION

People living with the aftereffects of a spinal cord injury (SCI) experience a loss of motor and sensory function based on the location and severity of the injury (Long and Lawton, 1955). A cervical SCI, the most common SCI level, causes the largest loss of function: tetraplegia. In New Zealand, cervical SCIs account for 44% of traumatic injuries (Rick Hansen Institute, 2018). Similarly, in the United States, 59% of new SCIs are sustained in the cervical region of the spine. This means that approximately 170,000 people are living with tetraplegia in the US alone (National Spinal Cord Injury Statistical Center, 2018). After sustaining a cervical SCI, several aspects of a person's life are impacted including limb and torso function, mobility, bowel and bladder function, and autonomic functions (Simpson et al., 2012). An injury or illness that has completely damaged the entire cross section of the spinal cord is classified as a complete injury. This type of injury results in complete paralysis of the legs, complete or partial paralysis of the torso and arms, and in the most severe cases, paralysis of the neck (Waters et al., 1991). An incomplete injury refers to partial damage to the spinal cord, resulting in limited reductions to sensory and motor functions (such as the ability to feel). A summary of the functional abilities and limitations of each cervical SCI is shown in Table 1.

Table 1. SCI motor level, muscle innervations and limitations
(Adapted from Floris et al.,(2002) and Bryden et al., (2012))

Motor Level	Upper Limb Muscle Innervated	Limitations
C5	Deltoid Biceps Brachialis Brachioradialis	No elbow extension Supinated forearm No wrist extension No active movement of fingers or thumb (Unable to use arm above shoulder level)
C6	Above muscle innervations plus: Clavicular head of Pectoralis Supinator Radial wrist extensor(s) (extensor carpi radialis longus; and/or extensor carpi radialis brevis)	No elbow extension No active movement of fingers or thumb (Unable to use arm above shoulder level without externally rotating)
C7	Above muscle innervations plus: Sternal head of Pectoralis Triceps Pronator teres Wrist flexor (flexor carpi radialis) Finger extension (extensor digitorum communis)	May have weak finger and/or thumb extension/flexion (Able to use arm above head in all positions)

Despite the challenges imposed through a loss of sensory and motor function, people living with an SCI want to live independent and meaningful lives (Snoek et al., 2004). To achieve independence and complete active daily living (ADL) tasks, people living with an SCI often rely on assistive and mobility devices. Due to the reduction in upper extremity function, innervated muscles are required to work harder to compensate. Frequent use of these muscles puts people living with an SCI at risk of developing upper extremity pain (Dalyan et al., 1999).

To develop appropriate designs to be used by all, the strength capabilities and limitations of people with reduced function must be well understood. To reduce the risk of developing upper extremity pain, it is recommended that the applied force of a repetitive task should not exceed one-third of an individual's maximum isometric strength (Das and Forde, 1999). Traditionally, previous studies have focussed on measuring the isometric force of the target population. This enables the force requirements and risk of repetitive injury to be evaluated and minimised through updating designs such that the force requirements are well below the individuals force exertion limits for a given position and direction.

Das and Forde (1999) completed isometric force measurement to improve the understanding of the single direction upper body strength capabilities of individuals with C4-T11 SCIs. Pull up and push

down tests were completed in a seated position using 24 positions to gather strength data to aid with the design of workspaces. The strength patterns of people with C5-C7 tetraplegia were investigated by Gooch et al. (2011) in greater detail using force contour plots on the sagittal plane. The results from this study highlighted a dramatic reduction in the upper extremity strength of individuals with an SCI compared to non-disabled individuals (Gooch et al., 2011). The results from this study were used to make a recommendation for an improved wheelchair design. To further improve the upper extremity function of individuals with a C5-C7 injury, multidirectional isometric tests were completed by Stilwell et al. (2019) using a testing apparatus with multidirectional load cells on each handle. Force polar plots were used to display force patterns for all directions in the sagittal plane. The initial results from one participant with C6 tetraplegia highlighted a dramatic reduction in both the range of motion and strength capabilities of a person with C6 tetraplegia compared to non-disabled individuals (Stilwell et al., 2019).

Human models are one tool that can be used to predict and evaluate the strength capabilities of the human body. A number of models have been developed to evaluate the force requirements of individuals with no disability. Using elbow and shoulder articulation strength data, a three-dimensional hand force capability model was developed for a seated individual (Schanne, 1972). Analysis of the results from the model showed that it under predicted the force capabilities at the hand. Chaffin (1997) developed a human model to predict the lower back forces required to complete manual exertions such as lifting heavy loads. Another study developed a musculoskeletal model within Opensim to predict the isometric force capabilities in 26 directions for a single arm posture. The predictions correlated well to the isometric force measurements recorded from physical testing (Hernandez et al., 2015).

To the best of our knowledge, no biomechanical models exist to enable the predictions of isometric strength for people with complete tetraplegia. To support the design of effective assistive devices without the need for physical testing, this study aims to develop a simple 2D biomechanical model to enable sagittal plane strength patterns to be evaluated for a person with C5-C7 injury in a seated position.

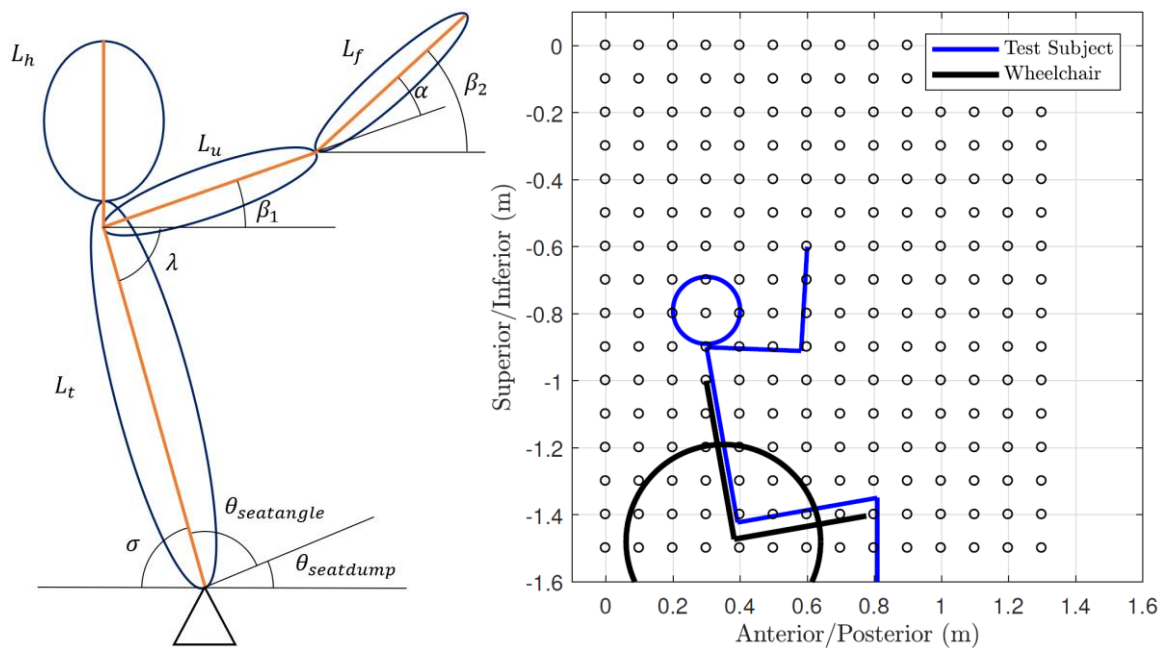
2 SETUP OF BIOMECHANICAL MODEL

2.1 Anthropometrics and structure

The biomechanical model was developed to predict human strength in the sagittal plane using a lateral view from the right-hand side of the body. The biomechanical model was set up using the 2D free body diagram (FBD) shown in Figure 1a. The FBD includes four rigid links (orange) to represent the head, torso, upper arm, and forearm. Angles σ , β_1 , β_2 , λ , $\theta_{seatangle}$, $\theta_{seatdump}$ and α define their orientations. Horizontal lines in Figure 1a are defined with respect to gravity. All joints are modelled as pin joints. For simplicity, the forearm and hand are assumed to be rigidly joined in a fixed position and connected to the test point of interest. This condition was used to match the physical testing conditions used by Stilwell et al. (2019), where participants with tetraplegia used grip assists to attach their hands to the test handle. The head and neck were assumed to be rigidly connected for the development of an initial model. Figure 1b shows the four rigid links implemented in the modelling environment in MATLAB with a defined hip position. This environment was defined based on the empirical test environment used by Stilwell et al. (2019), with the origin in the top left point. Each black circle represents a possible test point to be evaluated by the model. A simplified sketch to show the approximate position of the wheelchair and lower limbs have been included for clarity. The segment masses and lengths were defined using the total mass (m_{tot}) and body height (L_{tot}) of the model using body segment data from de Leva (1996), as detailed in Table 2.

Table 2. Definition of individual segment masses and lengths (de Leva, 1996)

Segment	Abbreviation	Total Mass (%)	Abbreviation	Total Height (%)
Head and Neck	m_h	6.94	L_h	11.7
Trunk	m_t	43.46	L_t	30.5
Upper Arm	m_u	2.71	L_u	16.2
Forearm and Hand	m_f	1.62 + 0.61	L_f	17.9
Thigh	m_{th}	14.16	L_{th}	24.3
Shank (and Foot)	m_l	4.33 (+ 1.37)	L_l	24.9



(a) FBD defining model variables (b) Subject at point (0.6,-0.6) in modelling environment

Figure 1. Basic FBD and MATLAB modelling environment

The location of the centre of mass (COM) of each segment was defined using the length definitions in Table 3. The distance to the COM of each segment were used to define the lengths of L_{fCOM} , L_{uCOM} and L_{tCOM} for the forearm, upper arm and torso, respectively.

Table 3. Definition of segment COM locations (de Leva, 1996)

Segment	Reference Point	Percentage of Segment Length to COM From Reference Point (%)
Head and Neck	Top of Trunk	48.98
Trunk	Bottom of Trunk	55.15
Upper Arm	Shoulder	57.72
Forearm and Hand	Elbow	45.74
Thigh	Hip	40.95
Shank	Knee	44.59

2.2 Human constraints and range of motion bounds

To ensure that the biomechanical model only evaluated points with a realistic posture, the range of motion of the elbow and shoulder articulations were defined using limits defined by a study completed by Boone and Azen (1979), as shown in Table 4. The neutral position of the upper arm has been defined when it is parallel to the trunk. The neutral position of β_1 has been defined where the upper arm is in 90° flexion (as shown in Figure 1a). The values of λ and β_1 were calculated using Equation (1) and (2) below. The backrest angle from the horizontal, σ , was defined using Equation (3) based on the incline of the seat angle ($\theta_{seatdump}$) and the seat angle between the cushion of the seat and backrest ($\theta_{seatangle}$), as detailed in Figure 1a. Upper limb joint angles were calculated using inverse kinematics. Points were not evaluated if they were either not reachable or required joint angles outside the definitions in Table 4.

Table 4. Definition of normal shoulder and elbow range of motion (Boone and Azen, 1979)

Joint	Joint Angle	Range of Motion Limit($^\circ$)
Shoulder (Backward) Extension	λ_{min}	-62.3
Shoulder (Forward) Flexion	λ_{max}	166.7
Elbow Extension	α_{min}	0
Elbow Flexion	α_{max}	142.9

$$\lambda = \sigma + \beta_1 \quad (1)$$

$$\beta_2 = \alpha + \beta_1 \quad (2)$$

$$\sigma = 180 - \theta_{seatdump} - \theta_{seatangle} \quad (3)$$

2.3 Definition of limiting torques

To define the maximum limiting torques for each joint articulation, maximum isometric shoulder and elbow moments from [Rozendaal et al. \(2003\)](#) were used. The limit for the maximum trunk extension moment was defined using values from a study completed by [Harbo et al. \(2012\)](#). Each of the limiting torques values are detailed in Table 5. The limiting joint torques were updated for the shoulder and elbow articulations as a function of the joint angle using the equations defined in Table 6. These equations were developed using the predictive torque curves from [Bober et al. \(2002\)](#). To calculate the limiting forces for a non-disabled person, the limiting torque values defined in Table 5 for each articulation were used. As C5-C7 SCIs all have a loss of trunk function, a torque curve for trunk extension was not incorporated into the model. To approximate the reduction in strength for people with tetraplegia, the active muscle volumes for each joint articulation were defined for each injury level. These percentages were based on the values used by [Hollingsworth \(2010\)](#). The active muscle volumes have been represented as a percentage of non-disabled values.

Table 5. Maximum joint torques and SCI reductions based on involved muscle volume ([Rozendaal et al., 2003](#), [Harbo et al., 2012](#) and [Hollingsworth, 2010](#))

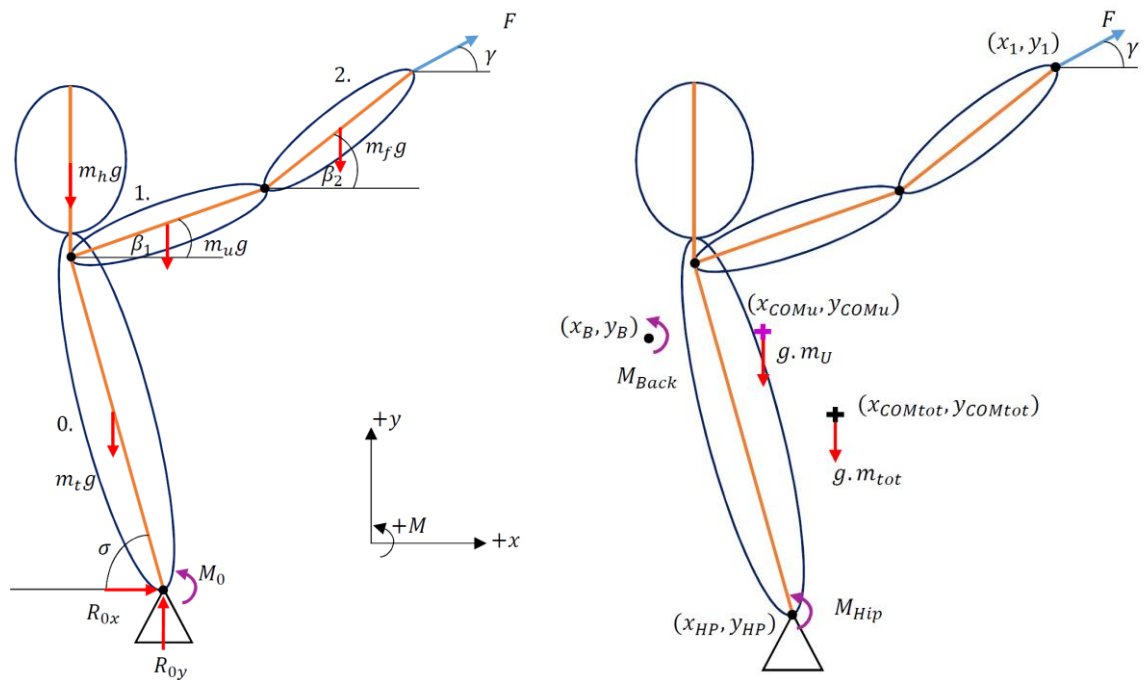
Joint Articulation	Abbreviation	Limiting Torque (Nm)	C5	C6	C7
Shoulder Extension	M_{1min}	-79	15.6%	50.5%	75.6%
Shoulder Flexion	M_{1max}	52	40.3%	85.5%	100%
Elbow Extension	M_{2min}	-43	0%	0%	50%
Elbow Flexion	M_{2max}	37	50%	100%	100%
Trunk Extension	M_{0max}	178.1	0%	0%	0%

Table 6. Predictive torque equations for maximum shoulder and elbow articulations

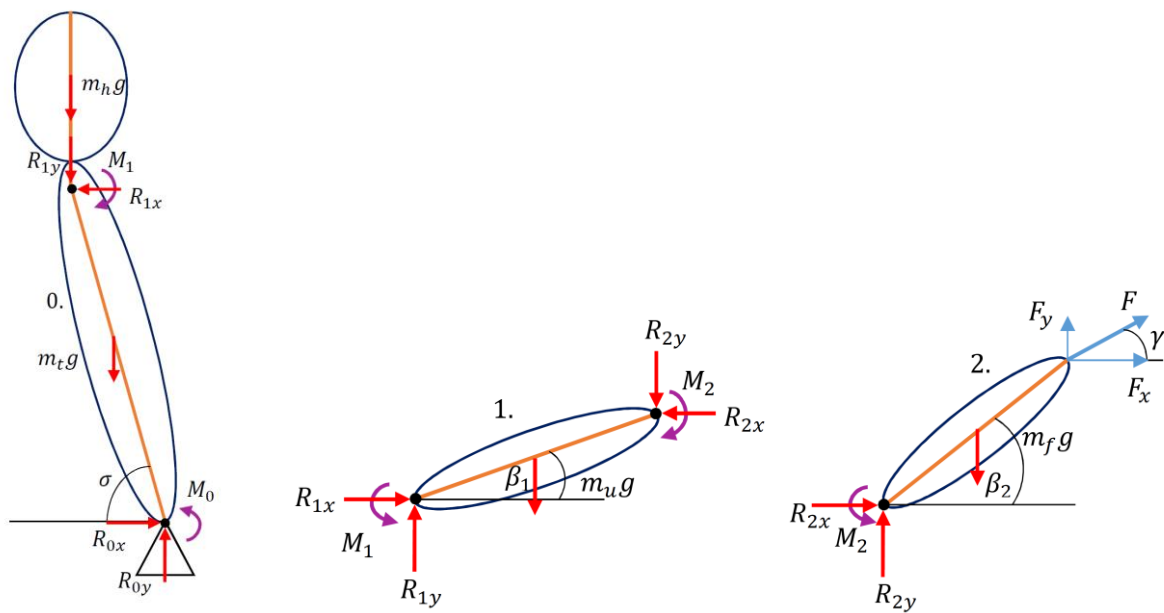
Joint	Torque Equations
Shoulder Extension	$0.0001247\alpha^3 - 0.0386657\alpha^2 + 3.6581774\alpha - 9.2731830$
Shoulder Flexion	$-0.0000998\alpha^3 + 0.0022541\alpha^2 + 1.0117515\alpha + 50.2801120$
Elbow Extension	$-0.0000248\lambda^3 - 0.0010131\lambda^2 + 0.7263628\lambda + 60.6928283$
Elbow Flexion	$-0.0003285\lambda^2 - 0.3587179\lambda + 86.0784486$

2.4 Development of equations used in biomechanical model

Using the FBDs in Figure 2, a number of equations were developed to approximate the maximum applied force at the hand for all directions in the sagittal plane. Figure 2a displays how a single force direction is defined as a function of gamma (γ), however, the model will evaluate all force directions in the sagittal plane. The definitions of F_x and F_y are shown in Equations (4) and (5). The positive x and y directions are defined in Figure 2a, with the positive x direction indicating direction where gamma (γ) is a value of 0° . This angle definition is used in subsequent polar plots. The amount of force required to pivot the upper body forward around the hip was defined as F_{hip} . The amount of force to pivot the total body mass backwards around the top of the backrest was defined as $F_{backrest}$. The static equilibrium equations for F_{hip} and $F_{backrest}$ were defined using Figure 2b, as detailed in Equations (6) and (7). These equations assume that the wheelchair is fixed in position. The equations for the reaction forces and moments of the torso, upper arm, and forearm were developed using the FBDs in Figure 2c, Figure 2d and Figure 2e, respectively. The resulting equations are included in Equations (8) - (16). These equations were used to calculate the force required for a single arm. The limiting force in the negative y direction was defined based on the total mass of the body, as detailed in Equation (17). The force required to overcome the friction of the seat ($F_{friction}$) and slide forward off the chair was defined in Equation (18) based on the angle of the seat (θ_{seat}) and a defined coefficient of friction (μ).



(a) FBD used to develop joint torque limits (b) FBD used to develop static equilibrium limits



(c) FBD of torso

(d) FBD of upper arm

(e) FBD of forearm

Figure 2. FBDs used to develop joint torque and static equilibrium limits of model

$$F_x = F \cos(\gamma) \quad (4)$$

$$F_y = F \sin(\gamma) \quad (5)$$

$$F_{hip} = \frac{g \cdot m_u \cdot (x_{HP} - x_{COMu}) + M_{Hip}}{2(\cos(\gamma) \cdot (y_1 - y_{HP}) - \sin(\gamma) \cdot (x_1 - x_{HP}))} \quad (6)$$

$$F_{backrest} = \frac{(x_{COMtot} - x_B) \cdot g \cdot m_{tot}}{2(\sin(\gamma) \cdot (x_1 - x_B) - \cos(\gamma) \cdot (y_1 - y_B))} \quad (7)$$

$$R_{2x} = -F_x \quad (8)$$

$$R_{2y} = -F_y + m_f \cdot g \quad (9)$$

$$M_2 = F_x \cdot L_f \cdot \sin(\beta_2) + \cos(\beta_2) (m_f \cdot g \cdot L_{fCOM} - F_y \cdot L_f) \quad (10)$$

$$R_{1x} = R_{2x} \quad (11)$$

$$R_{1y} = R_{2y} + m_u \cdot g \quad (12)$$

$$M_1 = M_2 + \cos(\beta_1) (L_u \cdot R_{2y} + m_u \cdot g \cdot L_{uCOM}) - \sin(\beta_2) \cdot R_{2x} \cdot L_u \quad (13)$$

$$R_{0x} = R_{1x} \quad (14)$$

$$R_{0y} = R_{1y} + g(m_h + m_t) \quad (15)$$

$$M_0 = M_1 - \cos(\sigma) (L_t(0.5 \cdot m_h \cdot g + R_{1y}) + (0.5 \cdot L_{tCOM} \cdot m_t \cdot g)) - L_t \cdot \sin(\sigma) \cdot R_{1x} \quad (16)$$

$$F_{selfweight} = 0.5 \cdot g \cdot m_{tot} \quad (17)$$

$$F_{friction} = \frac{g \cdot m_{tot} (\mu \cdot \cos(\theta_{seat}) + \sin(\theta_{seat}))}{2(\mu \cdot \sin(\gamma - \theta_{seat}) + \cos(\gamma - \theta_{seat}))} \quad (18)$$

2.5 Methodology used to evaluate force at hand

The model equations were implemented in MATLAB to evaluate the possible force outputs at the hand for the reachable points within the modelling environment. Polar plots of force were used to display the results from the model as they enable the magnitude of force to be displayed for all force directions in the sagittal plane in a single plot. The focus of the initial modelling was to investigate the impact injury level has on the polar plot shape. To do this, standard parameters were defined for all of the simulations. A total body mass and height of 73kg and 1.741m were defined based on values from [de Leva \(1996\)](#). A standard seat angle ($\theta_{seatangle}$) of 90°, seat dump angle ($\theta_{seatdump}$) of 10°, backrest position (x_B, y_B) of (0.3,-1), and shoulder position of (0.3,-0.9) were used for all injury levels. The following method was used to evaluate all points within the modelling environment:

1. The injury level was defined to ensure the correct reduction was applied to the joint torque limits.
2. Given a point in the modelling environment (x_1, y_1), the joint angles were determined using inverse kinematics. If the joint angles were outside the defined limit for natural joint angles, a force output of zero was recorded, and the next point in the modelling environment was evaluated.
3. The joint torque limits were adjusted based on the joint angles (α, λ), and specified injury level.
4. Each of the model limits were evaluated.
5. To display the results from all of the points within the modelling environment, the results from each point were filtered to only include the minimum force for a given direction. For directions where multiple limits overlapped, the lower force recording was used.

2.6 Assumptions used in biomechanical model

The development of the initial biomechanical model used a number of assumptions and simplifications. The assumptions relating to body mass, segment length, acceptable joint angles, and joint torque limits have been outlined in the description of the model setup. Further assumptions include:

- A coefficient of friction (μ) of 0.7 ([Moorthy and Kandhavdivu 2015](#)).
- Arms are assumed to have no abduction (parallel with sagittal plane).
- The wrist is assumed to be pronated.
- All segments remain in a fixed position for all force exertion directions.
- Arm strength is assumed to not be limited by wrist strength.
- The mass of the head is assumed to act in line with the shoulder.
- Results are shown for a single arm. It is assumed that each hand applies an even amount of force when calculating the hip/trunk, self-weight and friction limits.

3 HUMAN STRENGTH PREDICTIONS USING BIOMECHANICAL MODEL

The detailed strength predictions for a non-disabled and C7 injury level at a single point are shown in the polar plots in Figure 3. The polar plot includes lines for all limits implemented in the model. The filtered polar plot is highlighted in magenta. There is only one line for the hip limit as the equations based on joint torques and static equilibrium produced the same result. The filtered polar plots over the complete modelling environment for each injury level are shown in Figure 4. To improve the clarity of the filtered polar plots, a circular force scale and an outline of a wheelchair and body have been included.

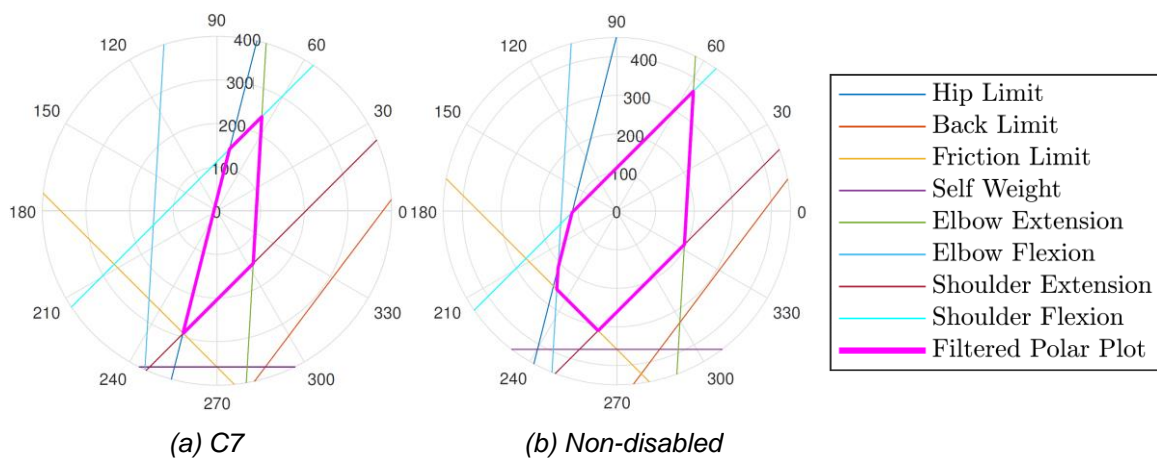


Figure 3. Detailed polar plot results for point (0.6,-0.6) showing all model limits

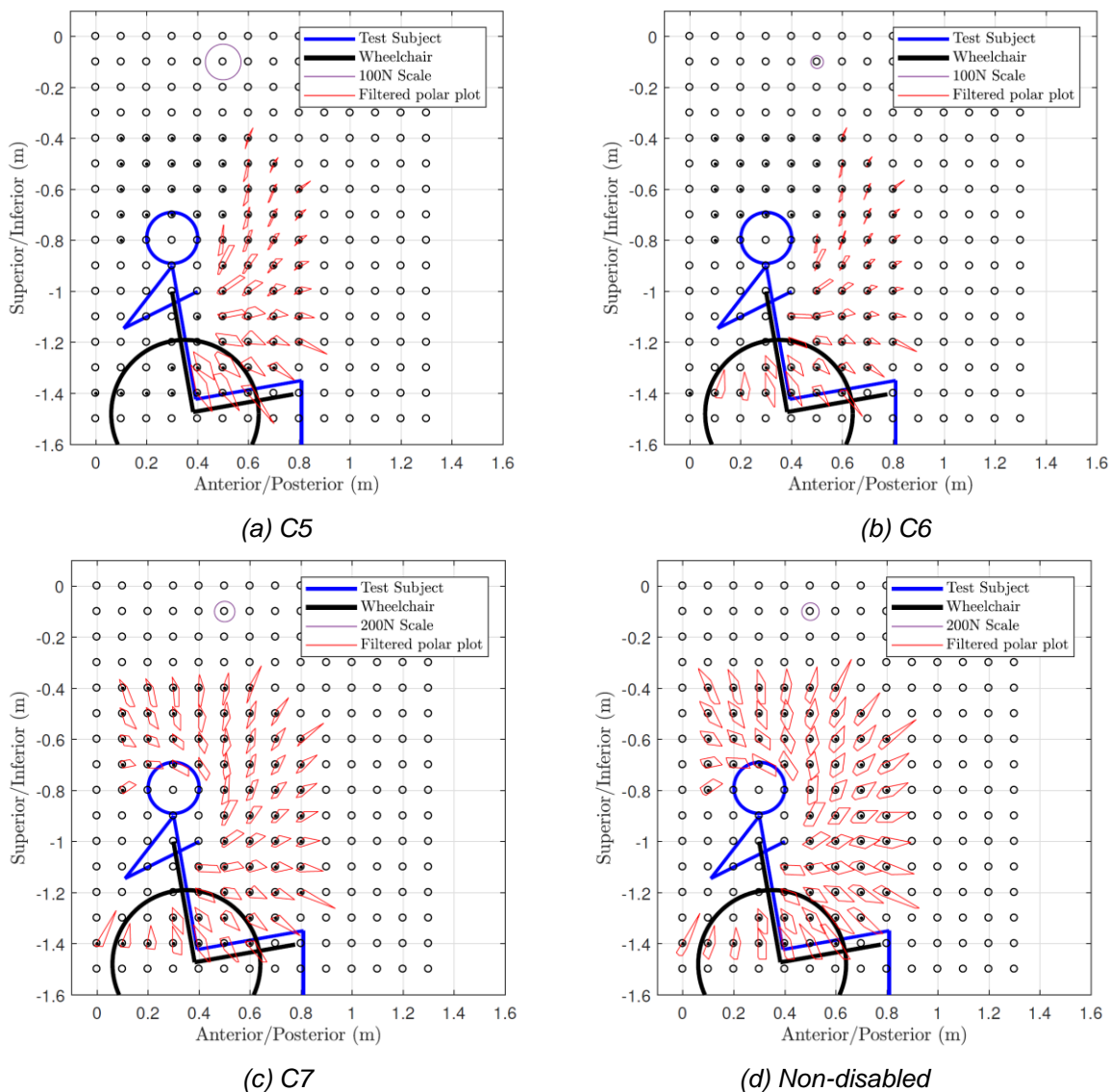


Figure 4. Filtered polar plots over the modelling environment for each injury level

4 DISCUSSION

The 2D biomechanical model developed in this paper has provided a simple method to evaluate multidirectional force in the sagittal plane at the hand throughout a person's range of motion in a seated position. The detailed polar plots give insight into the factors that cause the limits of applied force in specific directions. The limit lines in Figure 3 show that for point (0.6,-0.6) (shown in Figure 1b),

strength is limited by different limits depending on the direction. For example, the non-disabled result in Figure 3b shows that pushing forward in the 0° direction was limited by the elbow extension limit and that pushing upwards in the 90° direction was limited by the shoulder flexion limit. There is a considerable difference when this result is compared to the C7 polar plot in Figure 3a. Although pushing forward in the 0° direction is also limited by the elbow extension limit, the magnitude of force has halved in size from approximately 180 N to 90 N. This difference is a result of the 50% reduction in the elbow extension limit as defined in Table 5. The limiting factor for pushing upwards in the 90° direction is not the same as the limiting factor for the non-disabled result. The polar plot shows that pushing upwards is severely limited by the hip limit. This difference is caused by the lack of trunk function and control, as people with tetraplegia have no trunk function. This means that although the user may be physically able to apply a larger force in this direction, a force larger than the hip limit would cause the user to pivot at the hip and possibly fall out of their wheelchair. Comparing the biomechanical model polar plots to the polar plots gathered using empirical testing by Stilwell et al. (2019), the detailed polar plots generated from the 2D biomechanical model developed in this paper provide greater insights into the limiting factors that influence the magnitude and shape of a polar plot at a specific plot.

The filtered polar plots in Figure 4 highlight the impact reductions in joint strength have for people with C5-C7 tetraplegia compared to people with no disability. The trends of the filtered polar plot show that as the injury level increases from C7 to C5, both the number of reachable points and the magnitude of force in the reachable polar plots decreases. This result agrees with the trends previous empirical studies completed by Gooch et al. (2011) have found when measuring the isometric strength of people with tetraplegia. The reduction in magnitude is caused by the joint articulation limits defined in Table 5. However, the change in polar plot shape is not consistent for each injury level as the reductions in limiting torques are not linearly proportional to injury level. As injury level increases, the shape of the filtered polar plots tends towards a triangular shape. The triangular shape is caused by many points being limited by the combination of hip limit, shoulder extension limit, and elbow extension limit. This is caused by the reductions in the limiting joint torques becoming more significant as the injury level increases, as both the trunk extension and elbow extension limits being 0 Nm when modelling a C5 or C6 level injury. This reduction has a significant effect on the shape of the polar plots causing them to become increasingly thin. The lack of trunk stability has the most significant effect on force output in positions where the moment arm of applied force is large compared to the moment arm of the COM. This factor emphasises the importance of optimised wheelchair setup for people with tetraplegia. Changes to the wheelchair parameters can shift the COM of the user away from the hip joint.

The results in Figures 4a and 4b indicate that people with a C5 or C6 injury level cannot apply force at the "reachable" points above their head, as indicated by the points that have a black dot and no filtered polar plot. Although it is possible to reach these points using natural postures, the reductions in upper limb strength are reduced to the point where the self-weight of the arm causes the moment at the elbow (M_2) to be smaller the limit of 0 Nm. This means that at these positions, the moment at the elbow exceeds the elbow extension limit for all force directions. This result agrees with the limitations defined in Table 1 for C5 and C6 injury levels. Similarly, the C5 results display a number of points in the lower rear location where no force can be applied. In these positions, the resulting moment at the shoulder (M_1) and elbow (M_2), due to the self weight of the arm, exceed the elbow and shoulder extension limits.

Overall, the initial results have shown that the biomechanical model is a tool that can be used to aid designers evaluate their designs, such as workspaces or assistive devices, in terms of specific force requirements. Using the model, designers can optimise their designs to utilise areas and directions of high strength within a person's range of motion. Contrastingly, the model can also be used to identify areas and directions where applications of force for people with tetraplegia should be avoided.

The model developed in this paper is limited by the assumptions listed in Section 2.6. Although the assumptions enable a 3D system to be modelled in 2D space, they also limit the accuracy of the results. For example, the assumption that the arms are parallel to the sagittal plane is not correct for all test points. Often when people reach above their head they have their shoulders abducted and externally rotated. The inaccuracy in the assumptions for these points has a follow-on effect, as the limiting torque is set up to be a function of joint angle. The 2D biomechanical model also assumes standard body segment proportions based on height and limits for joint strengths. In reality, there will be variations in these parameters for different individuals, including variations in the strength of people with the same injury level and severity. Future work could look to create a 3D model that captures these parameters (strength limits, segment lengths and joint angles) more accurately.

5 CONCLUSION

This paper has presented a 2D biomechanical model that enables multidirectional force at the hand to be predicted for a person in a seated position. The results in this paper provide designers with a more detailed visual and quantitative method to evaluate multidirectional strength in the sagittal plane over a person's range of motion. The detailed polar plots provided further insights into the impact reduced function of the torso and upper limb articulations have on both the magnitude and direction of applied force at the hand for people with tetraplegia. The reduction in torso function for people with tetraplegia has a significant impact on the force required to pivot the upper body around the hip. The number of reachable points is also impacted by the reductions in strength for people with tetraplegia. The filtered polar plots show that the size and shape of the polar plots can vary widely between the different SCI levels. Overall, this 2D biomechanical model is a good starting point to enable strength patterns in the sagittal plane to be evaluated for a person with C5-C7 injury in a seated position.

REFERENCES

- Bober, T., Kulig, K., Burnfield, J.M. and Pietraszewski, B., 2002. Predictive torque equations for joints of the extremities. *Acta of Bioengineering and Biomechanics*, 4(2), pp.49-60.
- Boone, D.C. and Azen, S.P., 1979. Normal range of motion of joints in male subjects. *JBJS*, 61(5), pp.756-759.
- Chaffin, D.B., 1997. Development of computerized human static strength simulation model for job design. *Human Factors and Ergonomics in Manufacturing & Service Industries*, 7(4), pp.305-322.
- Dalyan, M., Cardenas, D. D. & Gerard, B. 1999. Upper extremity pain after spinal cord injury. *Spinal Cord*, 37, 191-195. <https://doi.org/10.1038/sj.sc.3100802>
- Das, B. & Forde, M. 1999. Isometric Push-up and Pull-down Strengths of Paraplegics in the Workspace: 1. Strength Measurement Profiles. *Journal of Occupational Rehabilitation*, 9, 277-289.
- De Leva, P. 1996. Adjustments to Zatsiorsky-Seluyanov's segment inertia parameters. *Journal of Biomechanics*, 29, 1223-1230. [https://doi.org/10.1016/0021-9290\(95\)00178-6](https://doi.org/10.1016/0021-9290(95)00178-6)
- Gooch, S., Medland, T., Rothwell, A., Dunn, J. & Falconer, M. On the design of devices for people with tetraplegia. DS 68-4: Proceedings of the 18th International Conference on Engineering Design (ICED 11), Impacting Society through Engineering Design, Vol. 4: Product and Systems Design, Lyngby/Copenhagen, Denmark, 15.-19.08. 2011, 2011.
- Harbo, T., Brincks, J. & Andersen, H. 2012. Maximal isokinetic and isometric muscle strength of major muscle groups related to age, body mass, height, and sex in 178 healthy subjects. *Eur J Appl Physiol*, 112, 267-75.
- Hernandez, V., Rezzoug, N. & Gorce, P. 2015. Toward isometric force capabilities evaluation by using a musculoskeletal model: Comparison with direct force measurement. *Journal of Biomechanics*, 48, 3178-3184. <https://doi.org/10.1016/j.jbiomech.2015.07.003>
- Hollingsworth, L. 2010. Understanding and modelling manual wheelchair propulsion and strength characteristics in people with C5-C7 tetraplegia: a thesis submitted for the degree of Doctor of Philosophy, Bioengineering, the University of Canterbury. Dissertation/Thesis. <http://dx.doi.org/10.26021/3379>
- Long, C. I. & Lawton, E. B. 1955. Functional significance of spinal cord lesion level. *Arch Phys Med Rehabil*, 36, 249-55.
- Moorthy, R. R. & Kandhavadi, P. 2015. Surface friction characteristics of woven fabrics with nonconventional fibers and their blends. *Journal of Textile and Apparel, Technology and Management*, 9.
- National Spinal Cord Injury Statistical Center 2018. Spinal cord injury: Facts and Figures at a Glance. The University of Alabama at Birmingham, USA.
- Rick Hansen Institute 2018. New Zealand Spinal Cord Injury Registry Annual Summary Report 2016/17.
- Rozendaal, L. A., Veeger, H. E. J. & Van Der Woude, L. H. V. 2003. The push force pattern in manual wheelchair propulsion as a balance between cost and effect. *Journal of Biomechanics*, 36, 239-247.
- Schanne, F. J. 1972. A Three-Dimensional Hand Force Capability Model for a Seated Person. (Volumes I And II), University of Michigan.
- Simpson, L. A., Eng, J. J., Hsieh, J. T. C., Wolfe & The Spinal Cord Injury Rehabilitation Evidence Research Team, D. L. 2012. The Health and Life Priorities of Individuals with Spinal Cord Injury: A Systematic Review. *Journal of Neurotrauma*, 29, 1548-55. <http://dx.doi.org/10.1089/neu.2011.2226>
- Snoek, G. J., Ijzerman, M. J., Hermens, H. J., Maxwell, D. & Biering-Sorensen, F. 2004. Survey of the needs of patients with spinal cord injury: impact and priority for improvement in hand function in tetraplegics. *Spinal Cord*, 42, 526-532. <https://doi.org/10.1038/sj.sc.3101638>
- Stilwell, G., Symons, D., Gooch, S. & Dunn, J. Measurement of Multidirectional Arm Strength for People in a Seated Position. ASME 2019 International Design Engineering Technical Conferences and Computers and Information in Engineering Conference, 2019. V006T09A013.
- Waters, R.L., Adkins, R.H. and Yakura, J.S., 1991. Definition of complete spinal cord injury. *Spinal Cord*, 29(9), pp.573-581. <https://doi.org/10.1038/sc.1991.85>